**Supporting Information**

# Enhanced Electrochemical Performance of S,N-Containing Carbon Materials Derived from Covalent Triazine-Based Frameworks with Tetrathiafulvalene core

Arijit Maity,[a] Anupam Jana,[a] Sandeep Kumar Dey,[b] Christoph Janiak[*c] and Asamanjoy Bhunia[*a]

[a]Department of Chemistry, Inorganic Chemistry Section, Jadavpur University, Kolkata, 700032, India. E-mail: abhunia.chemistry@jadavpuruniversity.in.

[b]Material Science and Technology Division, CSIR-North East Institute of Science and Technology, Jorhat, Assam 785006, India.

[c]Institut für Anorganische Chemie und Strukturchemie, Heinrich-Heine-Universität

Düsseldorf, 40204 Düsseldorf, Germany.

**Synthesis of 2, 3, 6, 7-tetra(4-cyanophenyl)tetrathiafulvalene (TTFCN)**

$Pd(OAc)_2$ (84 mg, 0.38 mmol), $P^tBu_3$•$HBF_4$ (326 mg, 1.1 mmol), and $Cs_2CO_3$ (2.4 g, 7.5 mmol) were placed in a 50 mL reaction flask under Argon. THF (10 mL) was added and the mixture was stirred for 10 min. A solution of tetrathiafulvalene (307 mg, 1.5 mmol) and 4-bromobenzonitrile (1.4 g, 7.5 mmol) in THF (10 mL) was added. Then, the mixture was reflux for 15 h. The organic compounds were extracted with dichloromethane three times. The combined organic part was washed with brine, dried over anhydrous $Na_2SO_4$, and concentrated in vacuo. Chromatographic purification on silica gel by using hexane/dichloromethane as an eluent afforded TTFCN (668 mg) as a dark red solid. Yield: 70%. $^1$H NMR (DMSO-$d_6$): δ = 7.83 (dt, 8H), 7.42 (dt, 8H) (Fig. S15). $^{13}$C NMR ($CDCl_3$): δ = 108.52, 112.91, 118.05,129.60, 129.91, 132.76, 136.23 (Fig. S16).

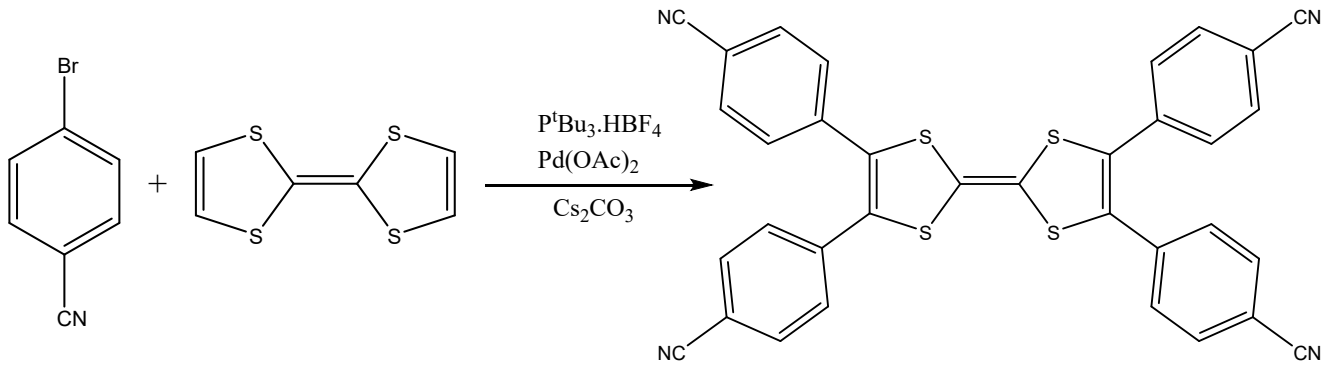


**TTFCN**

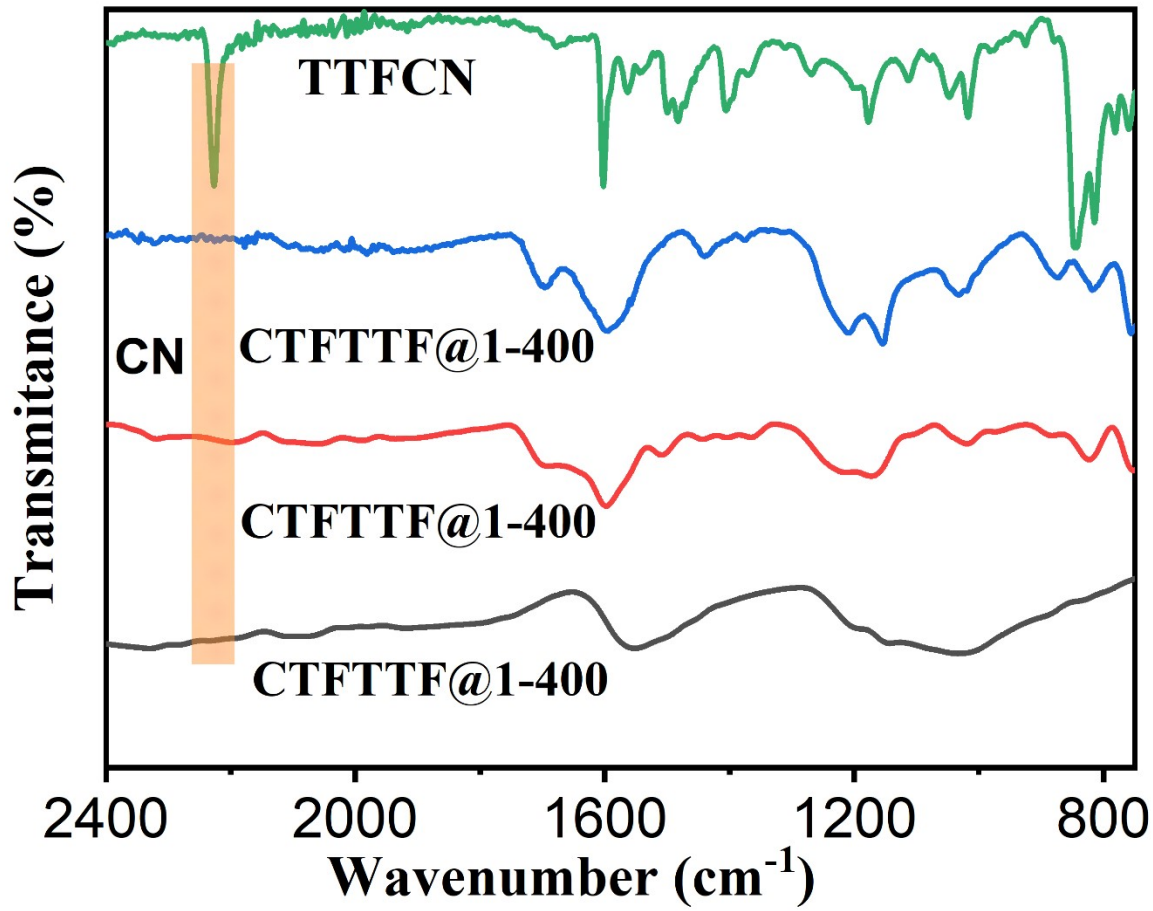


**Fig. S1:** IR spectra of monomer TTFCN and all three CTFs.

**Table S1:** CHN analysis of CTFs

| CTFs | Calculated | | | | Experimental | | | |
|---|---|---|---|---|---|---|---|---|
| | C | H | N | S | C | H | N | S |
| CTFTTF@1-400 | 67.08 | 2.65 | 9.20 | 21.63 | 65.829 | 3.813 | 1.352 | 4.037 |
| CTFTTF@2-400 | 67.08 | 2.65 | 9.20 | 21.63 | 67.751 | 3.221 | 0.485 | 3.141 |
| CTFTTF @2-700 | 67.08 | 2.65 | 9.20 | 21.63 | 57.351 | 2.836 | 1.7063 | 1.765 |

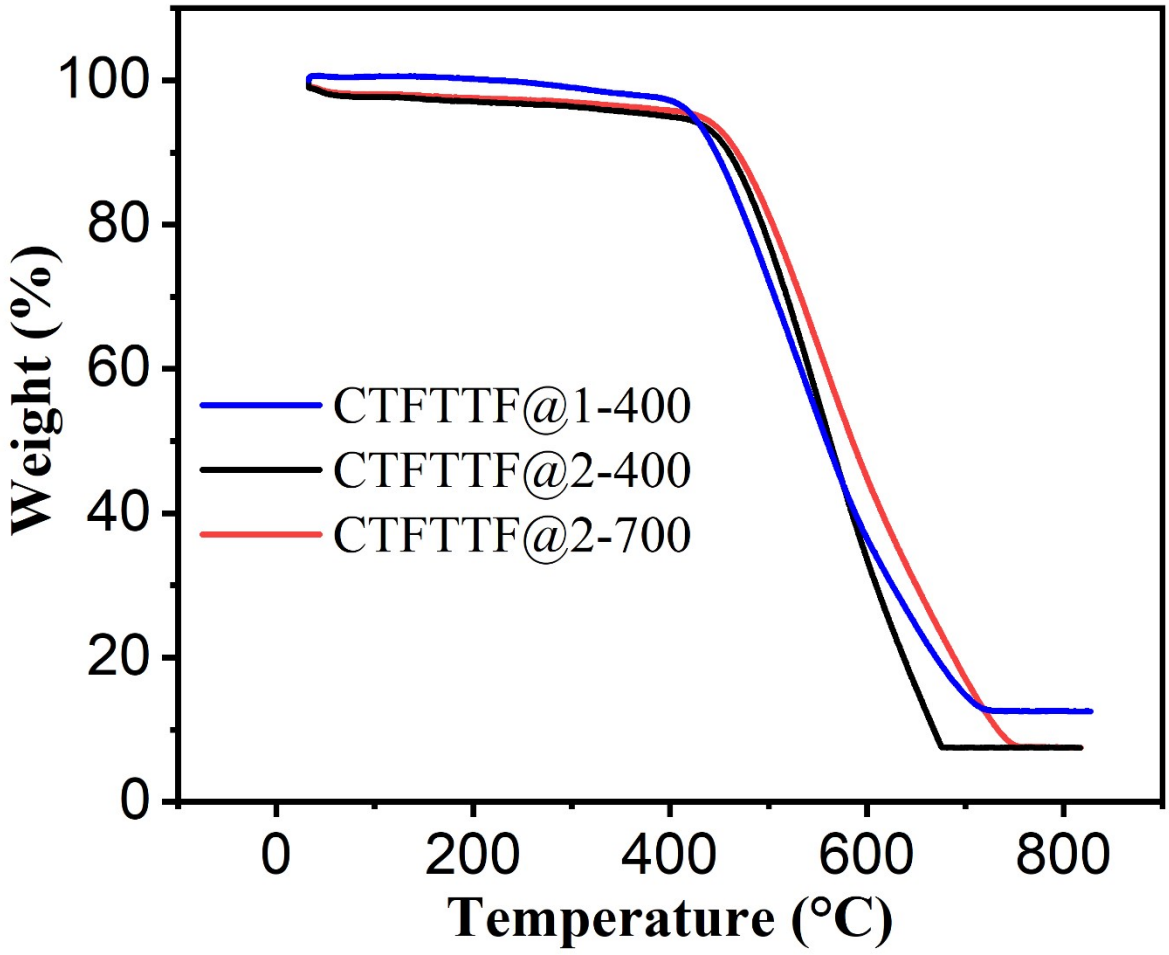


**Fig. S2**: TGA of all three CTFs.

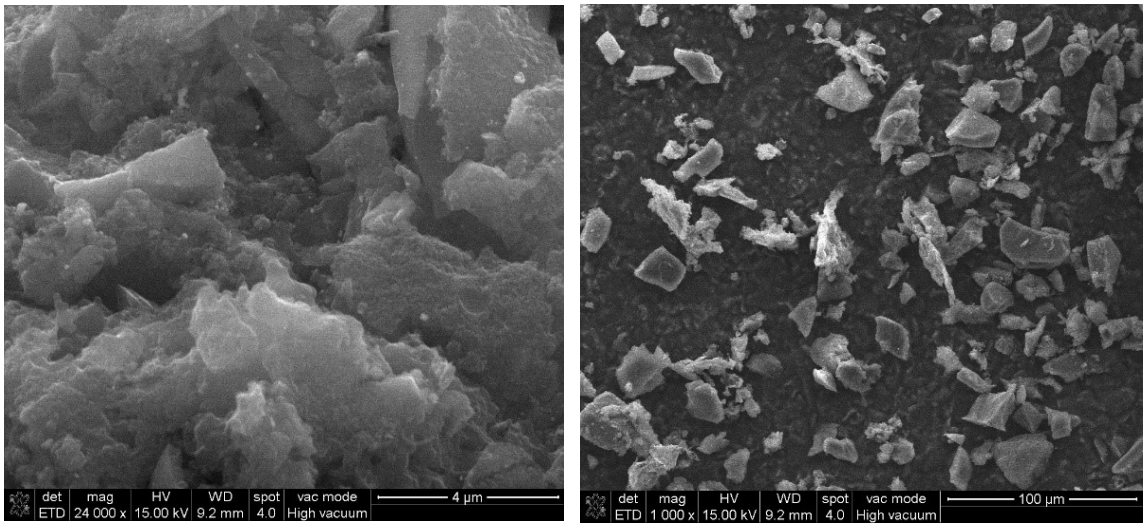


**Fig. S3**: SEM images of CTFTTF@2-400

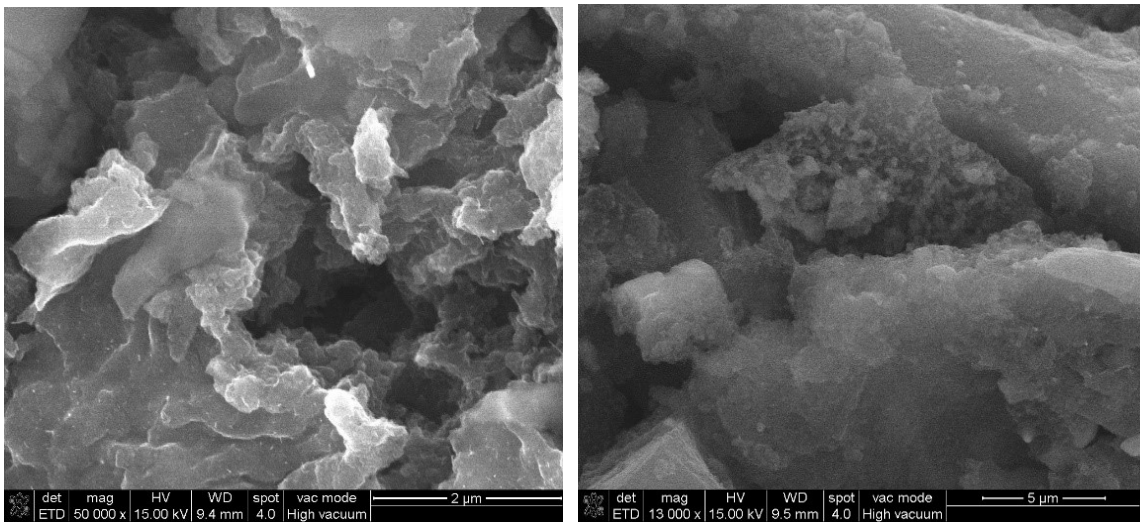


**Fig. S4**: SEM images of CTFTTF@2-700

Furthermore, transmission electron microscopy (TEM) was performed to provide a more detailed examination of the pore structure of the materials.

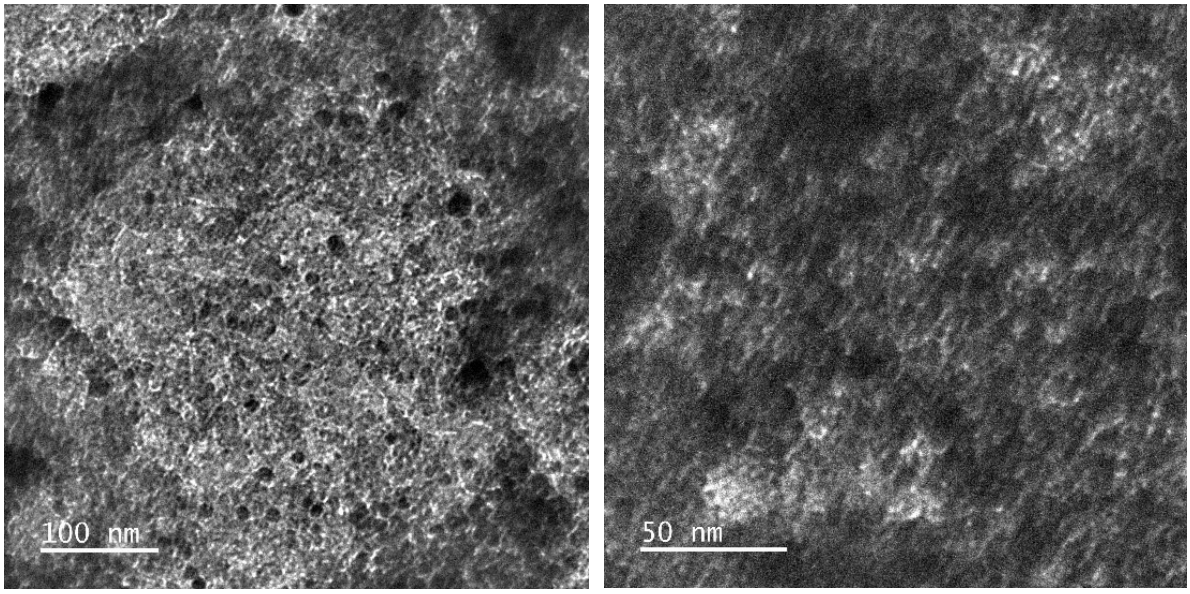


**Fig. S5**: TEM images of CTFTTF@2-400 (left side) and CTFTTF@2-700 (right side).

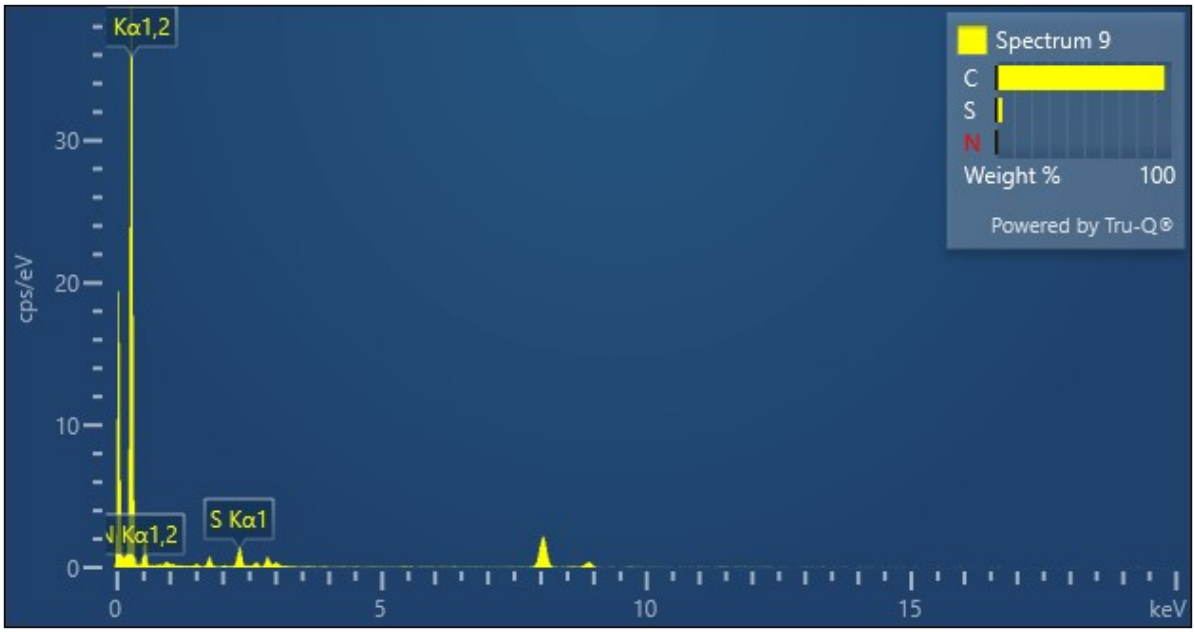


| Spectrum 9 | | |
|---|---|---|
| Element | Wt% | Wt% Sigma |
| C | 95.96 | 0.32 |
| N | 0.60 | 0.28 |
| S | 3.44 | 0.17 |
| Total: | 100.00 | |

| Spectrum 9 | | | | | | | |
|---|---|---|---|---|---|---|---|
| Element | Line Type | k Factor | k Factor type | Absorption Correction | Wt% | Wt% Sigma | Atomic % |
| C | K series | 1.879 | Theoretical | 1.00 | 95.96 | 0.32 | 98.16 |
| N | K series | 2.445 | Theoretical | 1.00 | 0.60 | 0.28 | 0.52 |
| S | K series | 1.110 | Theoretical | 1.00 | 3.44 | 0.17 | 1.32 |
| Total: | | | | | 100.00 | | 100.00 |

**Fig. S6:** EDX of CTFTTF@2-400


| Spectrum 3 | | |
|---|---|---|
| Element | Wt% | Wt% Sigma |
| C | 97.05 | 0.38 |
| N | 1.65 | 0.36 |
| S | 1.30 | 0.12 |
| Total: | 100.00 | |

| Spectrum 3 | | | | | | | |
|---|---|---|---|---|---|---|---|
| Element | Line Type | k Factor | k Factor type | Absorption Correction | Wt% | Wt% Sigma | Atomic % |
| C | K series | 1.879 | Theoretical | 1.00 | 97.05 | 0.38 | 98.08 |
| N | K series | 2.445 | Theoretical | 1.00 | 1.65 | 0.36 | 1.43 |
| S | K series | 1.110 | Theoretical | 1.00 | 1.30 | 0.12 | 0.49 |
| Total: | | | | | 100.00 | | 100.00 |

**Fig. S7:** EDX of CTFTTF@2-700

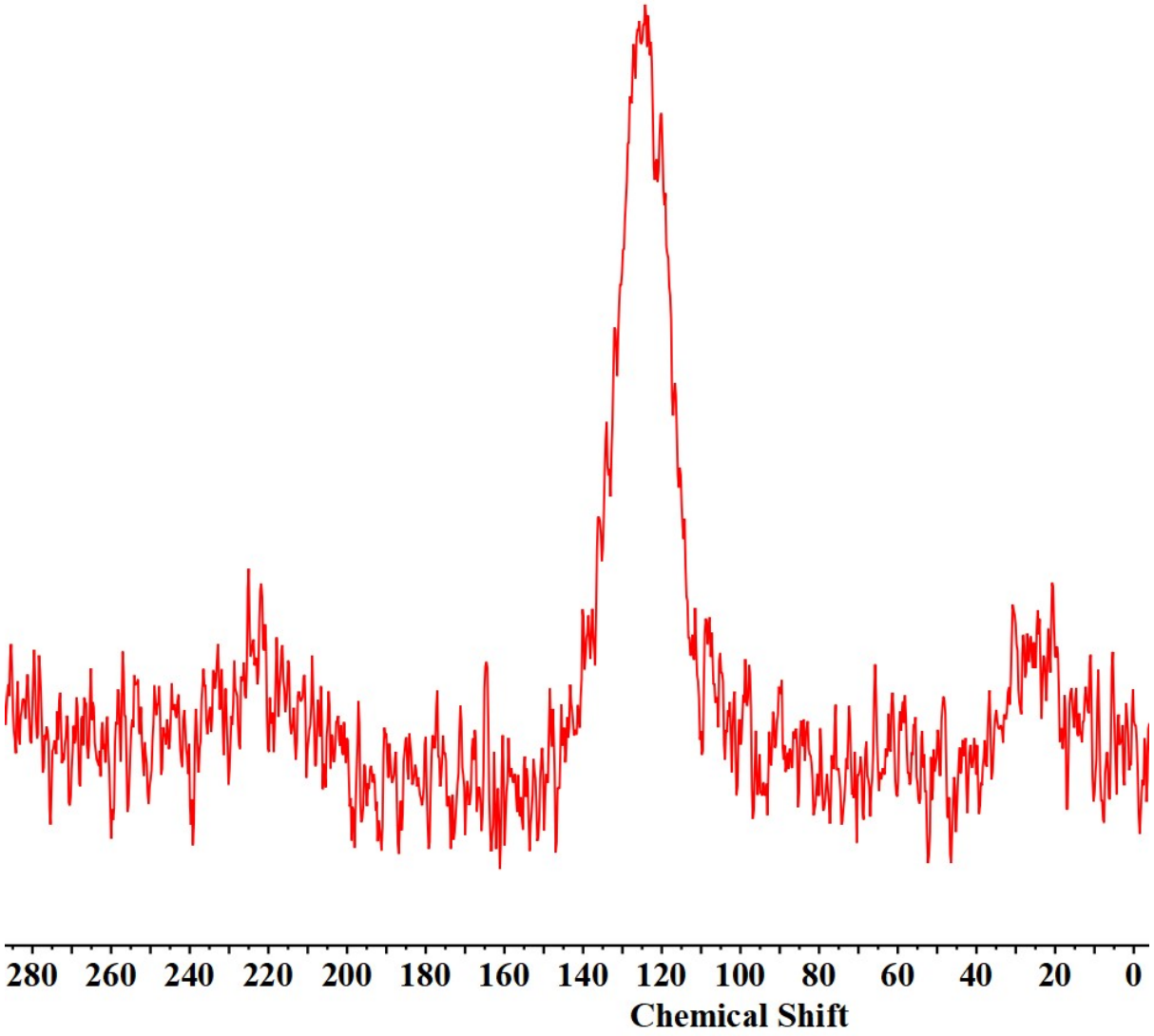


**Fig. S8:** Solid $^{13}C$ NMR of CTF@2-700.

In the present work, we measure solid-state MAS $^{13}C$ NMR spectra. However, we were unable to obtain meaningful spectra because these are graphene-like or similar to other carboneous materials. Another problem is that the CTFTTFs are also more conductive in nature. Rapid rotation of a conductive sample in a magnetic field will lead to strong heating of the sample and the rotor. As a result, there is a chance to damage inside the NMR instrument. It was still tried to measure the CTFTTF@2-700 sample by rotating them slowly at about 2-3 kHz instead of the normal 20-30 kHz with $^{13}C$-one pulse-experiments with decoupling and waiting times of 10 and 40 sec. Consequently, only a broad hump was seen from 100-160 ppm. Such a broad hump from 100 to 160 ppm without fine-structure resolution was also seen in the solid-state NMR, e.g., graphite oxide[1], graphene nanosheets[2], hydrothermally (from graphite oxide) reduced graphene sheets[3] or multi-walled carbon nanotubes[4]. Hence, similar to

graphene, no fine structure could be seen in the solid-state MAS $^{13}C$ NMR spectra of the samples.

**Table S2:** Amount of various type of nitrogen from XPS

| CTFTTFs | Pyridinic N (%) | Pyrrolic N (%) | Graphitic N (%) |
|---|---|---|---|
| CTFTTF@2-400 (400ºC | 35 | 44 | 21 |
| CTFTTF@2-700 (700ºC) | 12 | 20 | 68 |

**Electrochemical measurements**

CTFTTF@1-400, CTFTTF@2-400 and CTFTTF@2-700 coated GC electrodes CV curves, galvanostatic charge-discharge curves, and Nyquist plots were recorded individually using computerized CHI760E electrochemical workstation with three electrode system. Here, the counter electrode as platinum electrode, reference electrode as Ag/AgCl electrode and the working electrode is the glassy carbon modified CTFTTF@1-400, CTFTTF@2-400 and CTFTTF@2-700 electrode immersed in 1 M $Na_2SO_4$ solution as electrolyte.

The average specific capacitance of the obtained nanohybrid electrode was estimated using the CV as well as the charge-discharge patterns employing the formulas. (1) and (2).[5]

$$C_{sp} = \frac{\int I(V)dV}{2 * S * \Delta V * m} \rightarrow (1) \qquad C_s = \frac{2I * \Delta t}{m * \Delta V} \rightarrow (2)$$

Here, ∫I(V)dV: integral CV peak area, I: discharging current (mA), Δt: discharging time, ΔV: discharging voltage (V), and m: the electro-active mass (g) on the glassy carbon substrate.

The energy density (E,Whkg$^{-1}$)and power density (P, Wkg$^{-1}$) were calculated according to the equations (3) and (4)[6]

$$E = \frac{1}{2} \times C_s V^2 \times \frac{1}{4} \times \frac{1}{3.6} \longrightarrow \quad (3) \qquad P = \frac{E}{t} \longrightarrow \quad (4)$$

Where $C_s$ is the specific capacitance V is the cell voltage, and t is the discharging time(s).

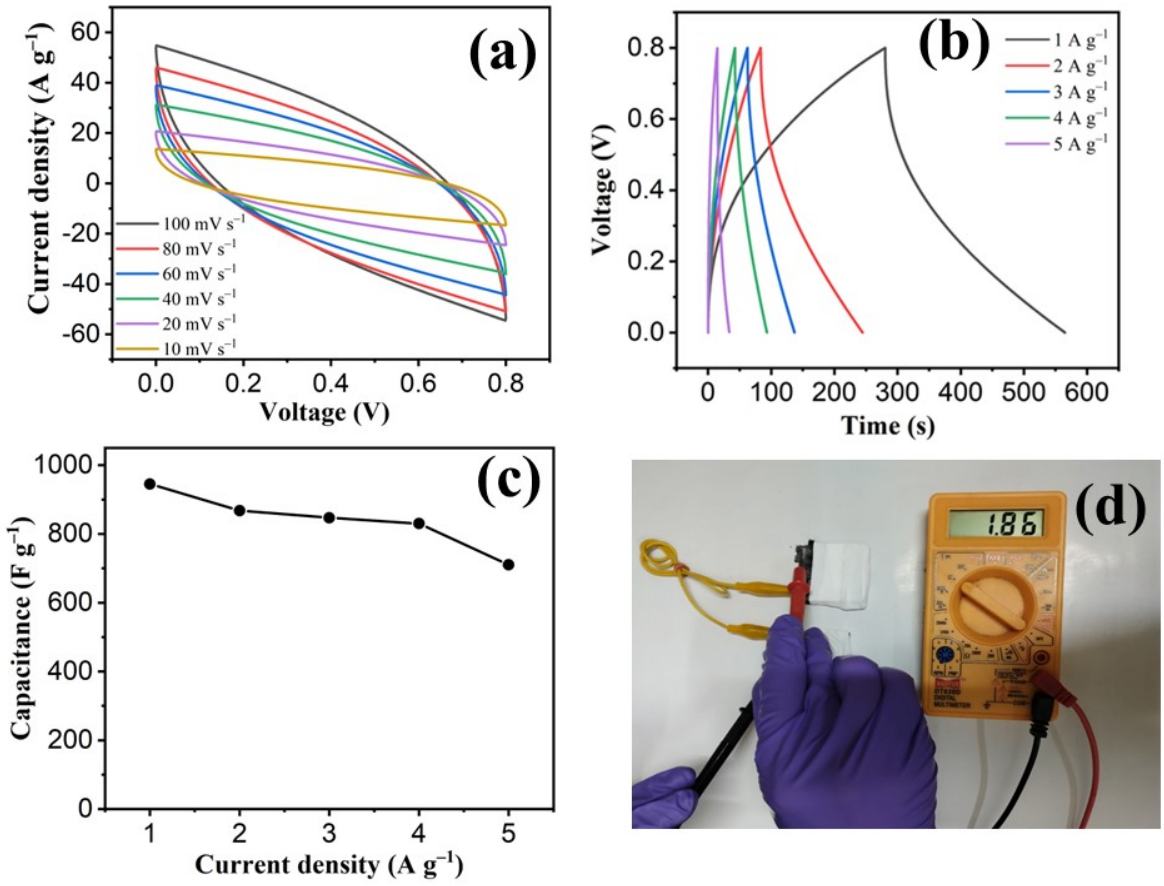


**Fig. S9**: (a) CV and (b) GCD curve of symmetrical device of CTFTTF (c) specific capacitance vs current density plots (d) Photograph of two proto-type devices connected in series.

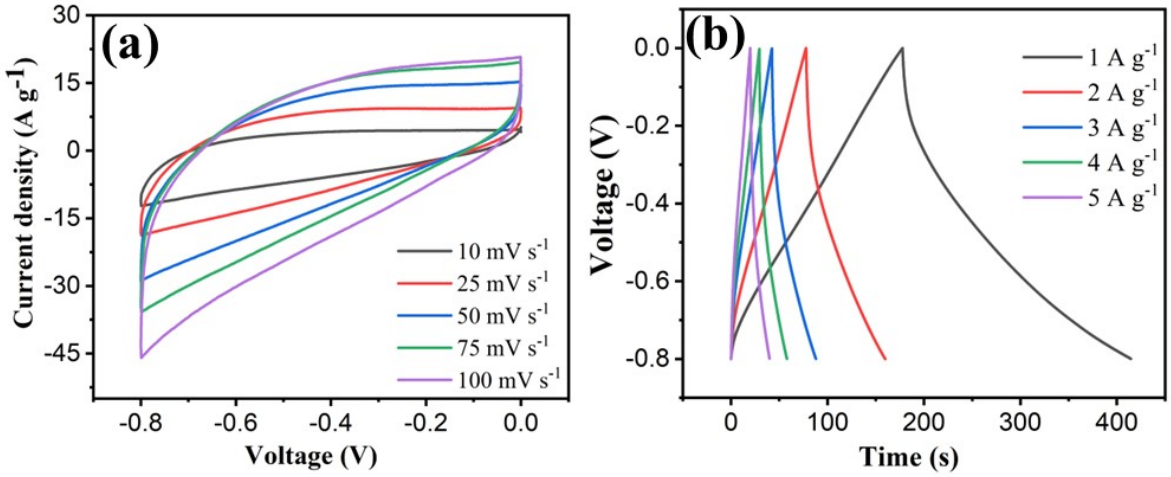


**Fig. S10.** (a) CV and (b) GCD curve of CTFTTF@2-700 in 1M KOH solution

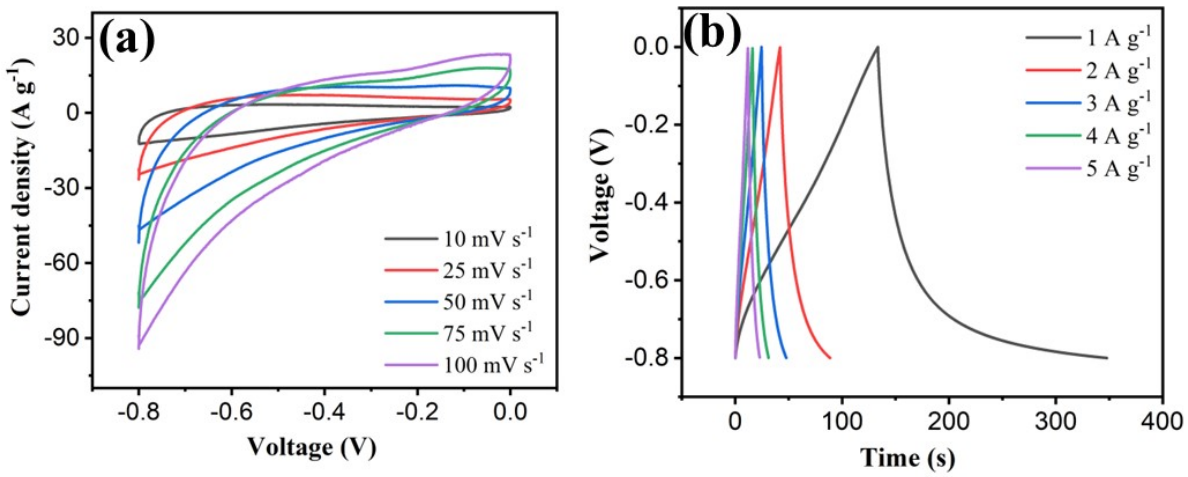


**Fig. S11**. (a) CV and (b) GCD curve of CTFTTF@2-400 in 1M KOH solution.

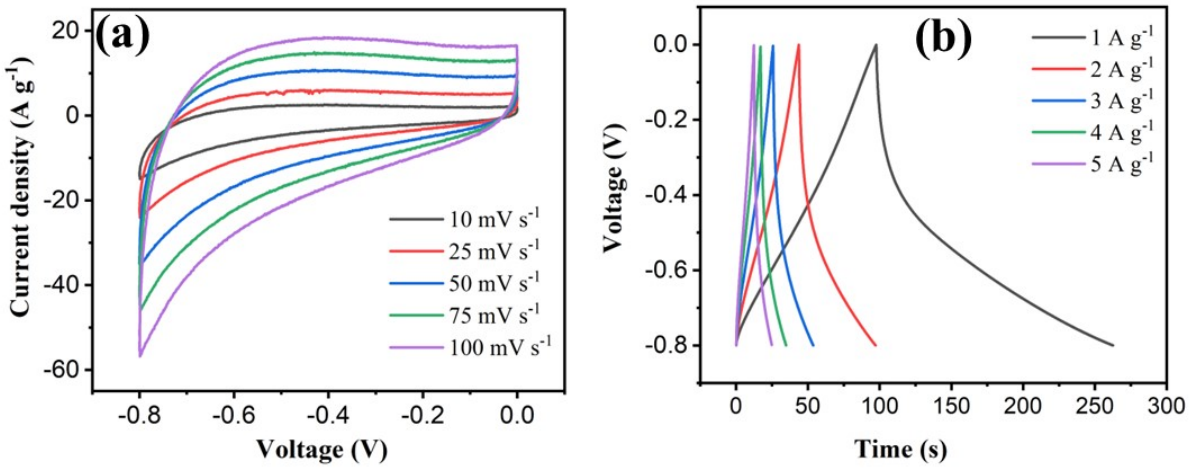


**Fig. S12**. (a) CV and (b) GCD curve of CTFTTF@1-400 in 1M KOH solution.

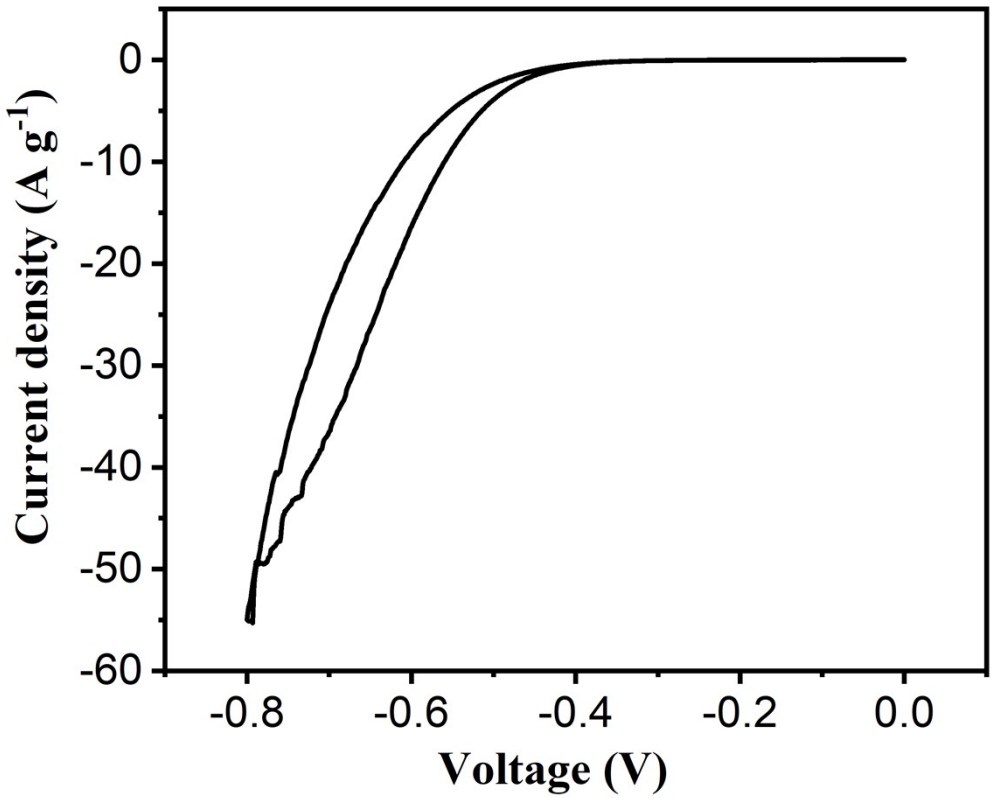


**Fig. S13:** CV curve of CTFTTF@2-700 in 1M $H_2SO_4$ solution.

**Table S3:** Comparison of capacitance value in three-electrode system

| SL.No | **Materials** | **Electrolyte** | **Method** | **Specific capacitance (F $g^{-1}$)** | **Ref.** |
|---|---|---|---|---|---|
| 1 | TDFP-1 | 0.1 m $H_2SO_4$ | CV | 354 at 2 mV $s^{-1}$ | 7 |
| 2 | TCOP | 6.0 M KOH | GCD | 278 at 1 A $g^{-1}$ | 8 |
| 3 | PDC-MA-COF | 6 M KOH | GCD | 335 at 1 A $g^{-1}$ | 9 |
| 4 | TPT-DAHQ COF | 1 M KOH | GCD | 256 at 0.5 A $g^{-1}$ | 10 |
| 5 | CTF/$ZnCl_2$-700 | $ZnCl_2$ | GCD | 141 at 1 A $g^{-1}$ | 11 |
| 6 | CTF-900 | 6 M KOH | GCD | 287 at 1 A $g^{-1}$ | 12 |
| 7 | p-CTF-800 | 1 m $H_2SO_4$ | GCD | 400 at 1 A $g^{-1}$ | 13 |
| 8 | BPY-CTF | 1 M KOH | GCD | 393.6 at 0.5 A $g^{-1}$ | 14 |
| 9 | TCNQ-CTF | 1 M KOH | GCD | 380 at 1 A $g^{-1}$ | 15 |

| | | | | | |
|---|---|---|---|---|---|
| 10 | FCTF | 1 M KOH | GCD | 379 at 1 A $g^{-1}$ | 16 |
| 11 | CTF-4CN-1-CNO | 1 m $H_2SO_4$ | GCD | 495 at 1 A $g^{-1}$ | 17 |
| 12 | C-ZIF-8/PEDOT–PSS (8:1) | 3 M KCl | GCD | 149.4 at 1 A $g^{-1}$ | 18 |
| 13 | CTF-800 | 1 m $H_2SO_4$ | GCD | 628 at 0.5 A $g^{-1}$ | 19 |
| 14 | Pyrrolo[3,2-b]pyrrole based CTF | 1 M KOH | GCD | 638 at 1 A $g^{-1}$ | 20 |
| 15 | IITR-COF-1 | 0.5 M $K_2SO_4$ | GCD | 182.6 at 1 A $g^{-1}$ | 21 |
| 16 | COFTTA–DHTA-NH2-f-MWCNT | 1 M $Na_2SO_4$ | GCD | 127.5 at 1 A $g^{-1}$ | 22 |
| 17 | COFs/NH2–rGO | 1 M $Na_2SO_4$ | GCD | 533 at 0.2 A $g^{-1}$ | 23 |
| 18 | Hex-Aza-COF-2 | 1 M $Na_2SO_4$ | GCD | 280 at 1 A $g^{-1}$ | 24 |
| 19 | N-doped Porous Carbon | 1 M $Na_2SO_4$ | GCD | 324 at 0.05 A $g^{-1}$ | 25 |
| 20 | S-CNO | 1M $Na_2SO_4$ | CV | 257 at 1 A $g^{-1}$ | 26 |
| 21 | Conductive MOF (Cu-CAT) | 3M KCl | GCD | 202 at 1 A $g^{-1}$ | 27 |
| 22 | **CTFTTF@2-700** | **1M $Na_2SO_4$** | **GCD** | **943 at 1 A $g^{-1}$** | **This work** |

**Table S4:** Conductivity values of CTFTTF@1-400, CTFTTF@2-400 and CTFTTF@2-700.

| Materials | Conductivity (S $cm^{-1}$) |
|---|---|
| CTFTTF@2-700 | $6.4\times10^{-4}$ |
| CTFTTF@2-400 | $1.3\times10^{-5}$ |
| CTFTTF@1-400 | $9.0\times10^{-6}$ |

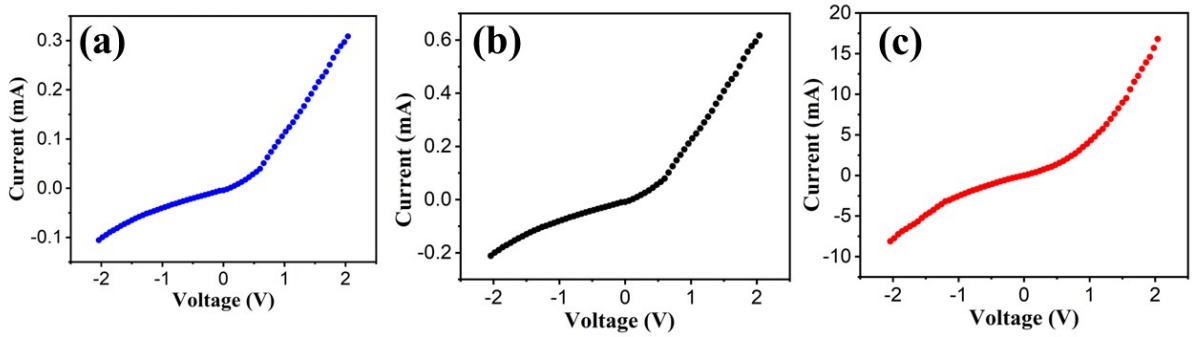


**Fig. S14:** I-V curve of (a) CTFTTF@1-400, (b) CTFTTF@2-400, (c) CTFTTF@2-700.

**Table S5:** Comparison of power density using two-electrode system

| SL. No | Electrode Materials | Electrolyte | Cell Voltage (V) | Energy Density (Wh $kg^{-1}$) | Ref. |
|---|---|---|---|---|---|
| 1. | CTF-800 | 1M $H_2SO_4$ | 1.0 | 15.5 | 16 |
| 2. | DCP-CTF-700 | 2.96 m $ZnCl_2$ | 1.0 | 3.76 | 8 |
| 3. | N-Carbon Framework | 1M $H_2SO_4$ | 1.0 | 7.5 | 28 |
| 4. | Porous Carbon | 6M KOH | 1.0 | 6.27 | 29 |
| 5. | ACS-4.0-800 Carbon | 6M KOH | 1.0 | 5.67 | 30 |
| 6. | Hex-Aza-COF-2 | 1 M $Na_2SO_4$ | 1.0 | 1.65 | 24 |
| 7. | S-CNO | 1 M $Na_2SO_4$ | 1.0 | 6.1 | 26 |
| 8. | N-doped Porous Carbon | 1 M $Na_2SO_4$ | 1.8 | 11.9 | 25 |
| 9. | $MnO_2$/CNT | 1 M $Na_2SO_4$ | 1.8 | 27 | 9 |
| **10.** | **CTFTTF@2-700** | **1M $Na_2SO_4$** | **0.8** | **15.7** | **Present Work** |

**NMR of Ligand TTFCN**

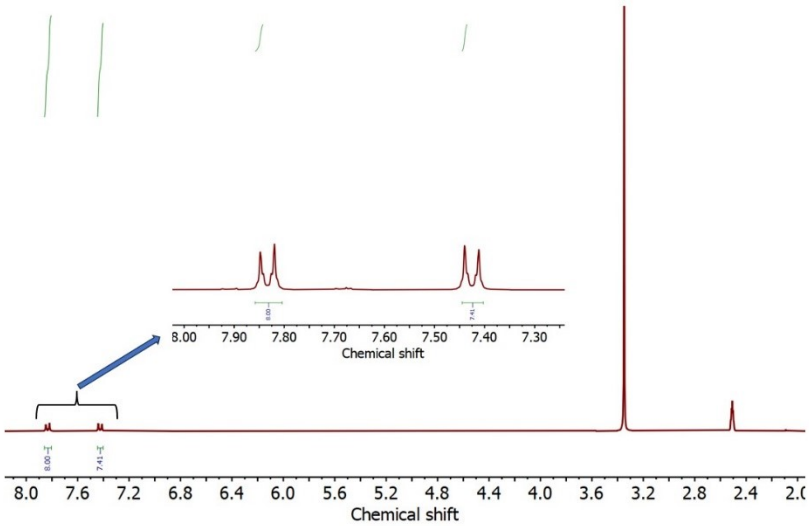


**Fig. S15**: $^{1}$H NMR spectrum (300 MHz) of TTFCN in DMSO-$d_6$.

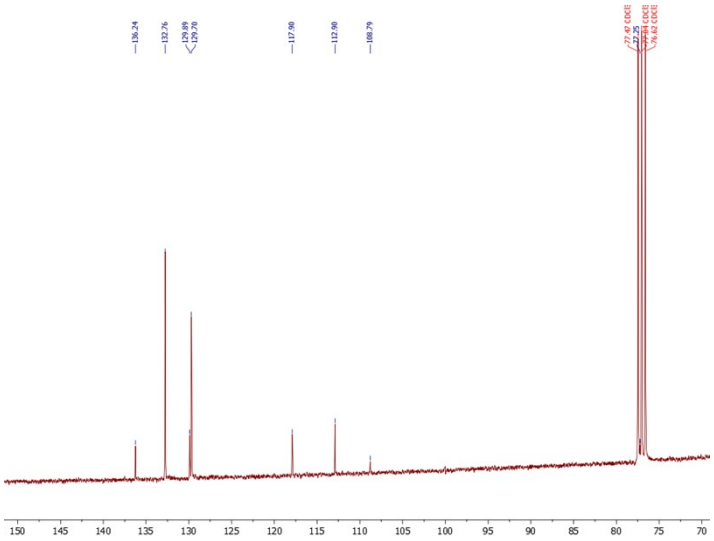


**Fig. S16:** $^{13}$C NMR spectrum (75 MHz) of TTFCN in $CDCl_3$.

**Reference**

1. L. B. Casabianca, M. A. Shaibat, W. W. Cai, S. Park, R. Piner, R. S. Ruoff and Y. Ishii, *J. Am. Chem. Soc*., 2010, **132**, 5672-5676.

2. X. Wang, Y. Hu, L. Song, H. Yang, W. Xing and H. Lu, *J. Mater. Chem*. A., 2011, **21**, 4222-4227.

3. D. Long, W. Li, L. Ling, J. Miyawaki, I. Mochida and S.-H. Yoon, *Langmuir*, 2010, **26**, 16096-16102.

4. E. Abou-Hamad, M.-R. Babaa, M. Bouhrara, Y. Kim, Y. Saih, S. Dennler, F. Mauri, J.-M. Basset, C. Goze-Bac and T. Wågberg, *Phys. Rev. B*, 2011, **84**, 165417.

5. V. K. Tiwari, Z. Chen, F. Gao, Z. Gu, X. Sun and Z. Ye, *J. Mater. Chem. A,* 2017, **5**, 12131−12143

6. M. Grundy and Z. Ye, *J. Mater. Chem. A,* 2014, **2**, 20316−20330.

7. P. Bhanja, K. Bhunia, K. S. Das, D. Pradhan, R. Kimura, Y. Hijikata, S. Irle and A. Bhaumik, *ChemSusChem*., 2017, **10**, 921–929.

8. M. Kim, P. Puthiaraj, Y. Qian, Y. Kim, S. Jang, S. Hwang, E. Na, W. S. Ahn, and S. E, Shim, *Electrochim Acta,* 2018*,* **284**, 98-107.

9. L. Li, F. Lu, R. Xue, B. Ma, Q. Li, N. Wu, H. Liu, W. Yao, H. Guo and W. Yang, *ACS Appl. Mater. Interfaces*, 2019, **11**, 26355–26363.

10. A. M. F. Mahdy, E. H. Y. Hung, T. H. Mansoure, H. H. Yu, T. Chen and S. W. Kuo, *Chem Asian J*., 2019, **14**, 1429-1435.

11. E. Troschke, D. Leistenschneider, T. Rensch, S. Grätz, J. Maschita, S. Ehrling, B. Klemmed, V. B. Lotsch, A. Eychmüller, L. Borchardt and L. S. Kaskel, *ChemSusChem*., 2020, **13**, 3192-3198.

12. B. Liu, J. Wen, H. Chen, M. Yang, Y. Liu and H. Li, *Batteries & Supercaps.,* 2020, **3**, 1091-1098.

13. C. Wu, H. Zhang, M. Hu, G. Shan, J. Gao, J. Liu, X. Zhou and J. Yang, *Adv. Electron. mater.,* 2020, **6**, 2000253.

14. Y. Zhang, B. Zhang, L. Chen, T. Wang, M. Di, F. Jiang, X. Xu and S. Qiao, *J. Colloid Interface Sci*., 2022, **606**, 1534-1542.

15. Y. Li, S. Zheng, X. Liu, P. Li, L. Sun, R. Yang, S. Wang, Z. S. Wu, X. Bao and W. Q. Deng, *Angew. Chem. Int. Ed*., 2017, **57**, 7992-7996.

16. Y. Gao, C. Zhi, P. Cui, K. I. A. Zhang, L. P. Lv and Y. Wang, *Chem Engineer J*., 2020, **400**, 125967.

17. A. Hryniewicka, J. Breczko, G. Siemiaszko, K. Brzezinski, A. Ilnicka, A. P. Terzykd and M. P. E. Plonska, *Mater. Adv.,* 2024, **5**, 1065-1077.

18. Y. Ko, J.Y. Lee, D. Kim, U. H. Lee and J. You, *ACS Appl. Electron. Mater.,* 2024, **6**, 1045-1054.

19. M. M. Vadiyar, X. Liu and Z. Ye, *ACS Appl. Mater. Interfaces,* 2019, **11**, 45805-4581.

20. A. Hryniewicka, J. Breczko, G. Siemiaszko, A. N. Papathanassiou, K.- G.Marek, K. A. Tarach, K. Brzezinski, A. Ilnicka, A. P. Terzyk, K. H. Markiewicz, L. Echegoyen and M. E. P. Brzezinska, *Sci Rep*, 2023, **13**, 10737.

21. Y. Kumar, I. Ahmad, A. Rawat, R. K. Pandey, P. Mohanty and R. Pandey, *ACS Appl. Mater. Interfaces,* 2024, **16**, 11605–11616.

22. B. Sun, J. Liu, A. Cao, W. Song and D. Wang, *Chem. Commun.,* 2017, **53**, 6303-6306.

23. P. Wang, Q. Wu, L. Han, S. Wang, S. Fang, Z. Zhang and S. Sun, *RSC Adv.,* 2015, **5**, 27290-27294.

24. S. Kandambeth, J. Jia, H. Wu, V. S. Kale, P. T. Parvatkar, J. Czaban-Jóźwiak, S. Zhou, X. Xu, Z. O. Ameur, E. Abou-Hamad, A.-H. Emwas, O. Shekhah, H. N. Alshareef, M. Eddaoudi, *Adv. Energy Mater.*, 2020, **10**, 2001673.

25. L. Guan, L. Pan, T. Peng, C. Gao, W. Zhao, Z. Yang, H. Hu, M. Wu, *ACS Sustain. Chem. Eng*., 2019, **7**, 8405-8412.

26. D. Mohapatra, G. Dhakal, M. S. Sayed, B. Subramanya, J.-J. Shim and S. Parida, *ACS Appl. Mater. Interfaces,* 2019, **11**, 8040–8050

27. W.-H. Li, K. Ding, H.-R. Tian, M.-S. Yao, B. Nath, W.-H. Deng, Y. Wang, G. Xu, *Adv. Funct. Mater.,* 2017, **27** 1702067.

28. H. Zhu, X. Wang, X. Liu and X. Yang, *Adv. Mater.,* 2012, **24**, 6524-6529.

29. H. Jiang, X. Ye, Y. Zhu, L. Wang, P. Zhao, Z. Yue, J. Xie, Z. Wan and C. Jia, *Appl. Surf. Sci*., 2019, **470**, 573-580.

30. D. Zhang, J. Zhao, C. Feng, R. Zhao, Y. Sun, T. Guan, B. Han, N. Tang, J. Wang, K. Li, J. Qiao, and

*J. Zhang, J. Power Sources*, 2017, **342**, 363-370.

31. D. Gueon and J.H. Moon, *ACS Sustainable Chem. Eng*., 2017, **5**, 2445–2453